HHS Public Access

Author manuscript

Mol Neurobiol. Author manuscript; available in PMC 2023 August 01.

Published in final edited form as:

Mol Neurobiol. 2022 August ; 59(8): 5104–5120. doi:10.1007/s12035-022-02905-4.

WDR5-HOTTIP histone modifying complex regulates neural migration and dendrite polarity of pyramidal neurons via reelin signaling

Minhan Ka[1], **Hyung-Goo Kim**[2], **Woo-Yang Kim**[3,*]

[1]Research Center for Substance Abuse Pharmacology, Korea Institute of Toxicology, Daejeon 34114, Republic of Korea

[2]Qatar Biomedical Research Institute, Hamid Bin Khalifa University, Doha, Qatar

[3]Department of Biological Sciences, Kent State University, Kent, OH 44242, USA

Abstract

WD-repeat domain 5 (WDR5), a core component of histone methyltransferase complexes, is associated with Kabuki syndrome and Kleefstra syndrome that feature intellectual disability and neurodevelopmental delay. Despite its critical status in gene regulation and neurological disorders, the role of WDR5 in neural development is unknown. Here we show that WDR5 is required for normal neuronal placement and dendrite polarization in the developing cerebral cortex. WDR5 knockdown led to defects in both entry into the bipolar transition of pyramidal neurons within the intermediate zone and radial migration into cortical layers. Moreover, WDR5 deficiency disrupted apical and basal polarity of cortical dendrites. Aberrant dendritic spines and synapses accompanied the dendrite polarity phenotype. WDR5 deficiency reduced expression of reelin signaling receptors, ApoER and VldlR, which were associated with abnormal H3K4 methylation and H4 acetylation on their promoter regions. Finally, an lncRNA, HOTTIP, was found to be a partner of WDR5 to regulate dendritic polarity and reelin signaling via histone modification. Our results demonstrate a novel role for WDR5 in neuronal development and provide mechanistic insights into the neuropathology associated with histone methyltransferase dysfunction.

[*]**Correspondence to**: Woo-Yang Kim, Ph.D., wkim2@kent.edu, PHONE: 402-559-1337.

Author contributions

M.K., H.K., and W.K. conceived, designed, and analyzed the experiments. M.K. and W.K. performed and wrote the paper. W.K. supervised the work.

Competing financial interests

Authors declare no financial interests.

Author Declarations

Ethics approval

Mouse handling and experimental procedures were reviewed and approved by the Institutional Animal Care and Use Committee (IACUC) of Kent State University (protocol #: 464 WK 18-08).

Consent to participate

Not applicable.

Consent for publication

All authors have consented to publication.

Research involving Human Participants and/or Animals

Not applicable.

Informed consent

Not applicable.

Keywords

WDR5; apical dendrite; dendritic spine; transcriptional regulation; histone modification

Introduction

Neurons are highly polarized cells with two functionally and morphologically distinct neurites, axon and dendrites [1,2]. Neurite polarization is a complex process, which takes place during neuronal migration and differentiation. Neurons migrate from their birthplace to their final position in the developing brain [3]. Apical and basal dendrites of cortical pyramidal neurons are established during migration [4]. After pyramidal neurons settle at appropriate positions, they further differentiate by creating extensive branches of apical and basal dendrites and forming spines to establish functional connectivity [5]. Abnormalities in dendritic polarity and arborization in a neural network lead to structural and functional brain defects, and are implicated in neurodevelopmental disorders such as autism and intellectual disability [6–9].

Transcriptional regulation by epigenetic mechanisms is a key process in brain development and essential to modulate neuronal morphology required for neural circuit formation in the brain [10]. Histones can be post-translationally modified by epigenetic mechanisms including acetylation and methylation and eventually modulate gene transcription [11,12]. WDR5 is a member of the WD40-repeat protein family and works for post-translational modifications on histone proteins [13,14]. As a core adaptor protein of the MLL histone methyltransferase (HMTs) complex, WDR5 participates in recruiting the HMT complex to histone H3K4 in target genes, leading to H3K4 tri-methylation [15,13]. Additionally, WDR5 directly associates with histone acetyltransferases (HATs) complexes and is required for acetylation at histone H4K16 [16]. WDR5-mediated H3K4 tri-methylation is necessary for HAT complex recruitment and the subsequent increase in acetylation of H4K16 [17].

WDR5 defects is involved in Kabuki Syndrome has been identified by multiple congenital abnormalities that mostly exhibit developmental delay, intellectual disability, autism [18]. Moreover, de novo mutation of WDR5 affects childhood apraxia of speech (CAS), also known as developmental verbal dyspraxia [19]. WDR5 is component of Complex Proteins Associated with Set1, also known as COMPASS which supports a link between histone methylation and chromatin remodeling during neurodevelopment [20]. X-linked mental retardation-linked CUL4B mutations resulted in the accumulation of WDR5 and H3K4 tri-methylation on the neuronal gene promoters and induce neurite extension [21].

We report that WDR5 is required for cortical neuronal positioning and dendrite polarity during brain development. Expression of reelin receptors is associated with the WDR5 function in neuronal development. In concert with other HMT factors such as HOXA transcript at the distal tip (HOTTIP), WDR5 epigenetically modifies histone molecules to influence reelin signaling and regulates neuron migration and dendrite differentiation. Our findings reveal a novel function of WDR5 in pyramidal neuron development in the brain.

Results

WDR5 is required for pyramidal neuron positioning in the developing brain

To explore the role of WDR5 in neuronal development, we first assessed WDR5 expression in the developing mouse brain. At embryonic day (E) 15.5, WDR5 was broadly expressed in the cerebral cortex (Figure 1A). However, at postnatal day (P) 14, WDR5 was highly accumulated at the upper layer (II-IV) of the cerebral cortex. In co-immunostaining of cortical sections with a NeuN antibody, WDR5 appeared to be expressed exclusively in neurons (Figure 1B). Co-labeling of WDR5 with a MAP2 antibody in cortical cultures confirmed the neuronal expression of WDR5 (Figure 1C). These results show that WDR5 is expressed in cortical neurons during embryonic and postnatal brain development, and suggest a potential role for the protein in neuronal development.

We tested whether WDR5 plays a role in neuronal placement during cerebrocortical development by examining the radial migration pattern of newly-born pyramidal neurons. We used the RNAi-mediated knockdown approach to silence WDR5 expression in embryonic pyramidal neural progenitors at the ventricular zone [22]. Either a plasmid encoding non-silencing shRNA (control) or shWDR5 was electroporated *in utero* into the ventricles of E14.5 brains. These shRNA constructs contain a GFP sequence in a separate reading frame to label transfected cells. Five days after electroporation (E19.5), most GFP-labeled pyramidal neurons migrated from the ventricular zone to the upper layer of the cortex in control brains (Figure 2A, 2B). However, radial migration of shWDR5-electroporated neurons was abnormal, as GFP-positive neurons were apparently localized throughout cerebral cortical regions including deeper layers V and VI. To exclude off-target effects of shRNAs, we generated a recombinant DNA that contains a shWDR5-resistant sequence (rWDR5) with twelve silent mutations (Figure 2C). To validate the rWDR5 construct, we co-transfected rWDR5 and shWDR5 in HEK 293T cells and measured WDR5 levels by Western blotting. Co-overexpression of rWDR5 suppressed shWDR5-mediated knockdown of WDR5 (Figure 2D). *In utero* co-electroporation of rWDR5 reversed the inhibitory effect of shWDR5 on radial neuronal migration (Figure 2E, 2F). Before migration, pyramidal neurons undergo a transition from a multipolar to a bipolar morphology stage in the intermediate zone [23,24]. WDR5 knockdown by shWDR5 markedly decreased the multipolar to bipolar transition of pyramidal neurons. Co-expression of rWDR5 rescued the abnormal transition caused by shWDR5 in the IZ (Figure 2E, 2G). Together, these data demonstrate that pyramidal neurons require WDR5 for their radial migration and bipolar morphogenesis during cortical development.

WDR5 regulates dendrite polarity in cortical pyramidal neuron

We investigated dendrite morphogenesis of pyramidal neurons in the control and WDR5-deficient condition after *in utero* electroporation of a control shRNA or shWDR5. In control brains, pyramidal neurons developed a single, long primary apical dendrite extending toward the pial surface, and several thin basal dendrites. However, WDR5-deficient neurons lost this long apical dendrite and developed several short dendrites (Figure 3A, 3B and Supplemental Figure 1A, 1B). *In utero* co-electroporation of rWDR5 rescued the inhibitory effect shWDR5 had on dendrite development (Figure 3A, 3B). The numbers of total and

primary apical dendrites were markedly increased in WDR5-deficent neurons compared to control pyramidal neurons (Figure 3C and Supplemental Figure 1C). Also, the lengths of primary apical and total apical dendrites were significantly decreased in WDR5-deficient neurons. However, the length of basal dendrites was increased in WDR5-deficient neurons. Co-expression of rWDR5 together with shWDR5 rescued the abnormal dendrite length and number in the shWDR5 condition. Additionally, we observed contrasting orientation patterns of apical and basal dendrites between control and WDR5-deficient neurons. Control neurons generally extended apical dendrites toward the pial surface, however, WDR5-deficient neurons showed wider angles of apical dendrite extension from the vertical midline, and developed multiple dendrites lacking specific orientation (Figure 3D). The orientation of basal dendrites did not appear to be different between control and WDR5-deficent neurons. But, WDR5-deficient neurons developed longer basal dendrites compare with control neurons (Figure 3D). Furthermore, WDR5-deficiency led to a decrease in the thickness of their main apical dendrites compared to those from control pyramidal neurons (Figure 3E, 3F). Next, we assessed dendritic development within cortical layer I. In control brains, dendritic tufts from layers II/III pyramidal neurons expanded into cortical layer I and attached to the pial surface of the cortex. However, in WDR5-deficient brains, dendritic branches of pyramidal neurons from layer II/III extended into layer I but did not anchor into the pial surface (Supplemental Figure 2A). The number of dendritic branches on the pial surface was markedly decreased in WDR5-deficient neurons while the branch number in layer I was increased, compared to the numbers in controls (Supplemental Figure 2B). Together, these results suggest a requirement for WDR5 in apical dendrite polarity and orientation in cortical pyramidal neurons during development.

Altered dendritic spines and synapses in WDR5-deficient neurons

Dendritic spines are small protrusions from dendrites that play critical roles in synaptic formation and transmission. Abnormal dendritic development in the WDR5-deficient condition led us to examined dendritic spines and synapses. Control or shWDR5 constructs were transfected into cultured cortical neurons at 5 DIV. Cultured neurons were fixed at 14 DIV and dendritic spines were assessed. Similar to the *in utero* electroporation findings, WDR5-deficient neurons in culture presented a decrease in the thickness of dendrites, compared to control neurons (Figure 4A, 4B). However, the number of dendritic spines was increased in WDR5-deficient neurons (Figure 4A, 4B). Abnormal spines were found in WDR5-deficient neurons as they were filopodia-like in appearance and did not form full-sized spine heads (Figure 4C, 4D). Next, excitatory and inhibitory synapses were investigated in control and WDR5-deficient neurons using immunostaining with antibodies to vGlut1 (excitatory) and vGAT (inhibitory). WDR5-deficient neurons exhibited an increase in the number of excitatory synapses compared to controls whereas they showed no change in the inhibitory synapse number (Figure 4E, 4F). As a result, the balance of excitatory and inhibitory synapses was impaired in the WDR5-deficient condition (Figure 4G). These results reveal that WDR5 is an important regulator of excitatory synapse formation and suggest that WDR5 dysfunction is linked to imbalanced neurotransmission.

WDR5 promotes expression of reeling signaling genes

Reelin signaling plays an essential role in dendrite growth and neurite orientation of cortical and hippocampal neurons [25,26]. Considering WDR5's established function in histone modification, we tested whether WDR5 influences transcription of reeling signaling genes. We first measured mRNA levels of reelin receptors ApoER and VldlR as well as relevant signaling components CDH2, LimK and CDK5 in cultured cortical neurons after WDR5 knockdown. The levels of ApoER, VldlR, LimK and CDK5 mRNAs were reduced in WDR5-deficient neurons, compared to those in control cells (Figure 5A, 5B). We also assessed other genes related to dendrite development. WDR5-deficient neurons showed reduced levels of BTBD3, NRG1, NPTN, AURKA and Shank3 mRNAs,, compared to controls (Figure 5A, 5B). Next, we examined whether WDR5 directly binds to target gene promoters (Figure 5C). We performed a ChIP assay with a WDR5 antibody followed by amplification of the ApoER or VldlR promoter region using PCR. We found that WDR5 indeed physically interacted with the ApoER or VldlR promoter (Figure 5D). We also investigated whether WDR5-deficiency affects epigenetic modification of histones at reelin receptor promoters. ChIP assay was performed using the methyl-H3, acetyl-H3 and acetyl-H4 antibodies combined with PCR. WDR5-deficient neurons showed decreased levels of acetylated Histone H3 and H4 at the target gene promoters compared to control neurons (Figure 5E–5H). Moreover, the level of tri-methyl-Histone H3K4 at the reelin receptor promoters was decreased in the mutant condition. However, the tri-methyl-Histone H3K9 level did not appear to be different between the control and WDR5-deficient condition.

WDR5 interacts with histone modifying proteins and lncRNA, HOTTIP in cortical neurons

We sought to identify WDR5 partners that form a histone modifying complex in the cerebral cortex. Cortical lysates were co-immunoprecipitated with a WDR5, ASH2L or KANSL1 antibody, and subsequently subjected to immunoblotting. We found that WDR5 was physically bound to ASH2L (Figure 6A). ASH2L belongs to the Set1/Ash2 HMT complex that specifically methylates Lys-4 of histone H3. The co-immunoprecipitation analysis also revealed that WDR5 interacted with a H4 HAT component, KANSL1 (Figure 6B). WDR5 has been shown to bind a gene expression enhancer, lncRNA HOTTIP [16,27]. Thus, we examined whether HOTTIP interacts with the WDR5 histone modifying complex by using the RNA immunoprecipitation (RNAIP) assay. We found that the lncRNA was a part of the histone modifying complex containing WDR5, ASH2L and KANSL1 (Figure 6C). Next, we tested whether WDR5 plays a role in the interaction between HOTTP and ASH2L. Using control and WDR5-deficient cortical cells, RNAIP was performed and resulted in a decreased binding affinity of the lncRNA and ASH2L (Figure 6D, 6E). WDR5 knockdown reduced the HOTTIP affinity to KANSL1 as well (Figure 6F, 6G). Finally, we assessed whether HOTTIP is required for the expression of reelin signaling components. In HOTTIP-deficient cortical neurons, the levels of ApoER and VldlR were decreased compared to the levels in control cells (Figure 6H, 6I). The ChIP assay showed that histone H4 acetylation was suppressed at the ApoER promoter in HOTTIP-deficient neurons (Figure 6J, 6K). The WDR5 association with the promoter was also decreased compared to the level in controls. Similarly, HOTTIP knockdown led to reductions in histone H4 acetylation and WDR5 binding at the VldlR promoter (Figure 6L, 6M).

HOTTIP regulates cortical dendrite arborization and polarity during development

We investigated the role of HOTTIP in dendrite development in cortical pyramidal neurons. We *in utero* electroporated either a control shRNA or shHOTTIP construct into E14.5 embryos and assessed dendritic morphology at P14. In control brains, pyramidal neurons developed a single, long primary apical dendrite extending toward the pial surface, and several short basal dendrites. However, HOTTIP-deficient neurons lost this long apical dendrite and instead showed several short apical dendrites (Figure 7A, 7B). The number of primary apical dendrites was markedly increased in HOTTIP-deficient neurons compared to the number in controls (Fgure 7C). The lengths of primary apical, total apical, and total dendrites were significantly decreased in HOTTIP-deficient neurons. However, the length of basal dendrites was increased in HOTTIP-deficient neurons. Furthermore, HOTTIP-deficient neurons did not develop apical dendritic tufts and showed wider angles of apical dendrite extension from the vertical midline (Figure 7D). These results suggest that HOTTIP is important of dendrite polarity and orientation in cortical pyramidal neurons.

Discussion

We provide evidence that WDR5 is required for dendrite outgrowth, polarity and dendritic spine formation in brain development. We also demonstrate that WDR5 and its lncRNA partner HOTTIP cooperatively play a key role in histone epigenetic modification to regulate reelin receptor expression. A schematic model of target gene regulation and dendrite polarity in the absence or presence of WDR5 is presented in Figure 8. Our findings provide insights into the pathogenic mechanism underlying WDR5-related neurodevelopmental disorders.

WDR5 is involved in cell morphology changes and differentiation [13].However, there has been no information available about the neuronal placement and polarity in which neurons find their destination and establish functional connections in the developing brain. We show that WDR5-deficient neurons are defective in neuronal migration during cortical development. Notably, WDR5-deficiency suppresses the multipolar-to-bipolar transition that is an essential step for pyramidal neurons to actively initiate radial migration [28,24]. The apical leading process of the bipolar extension renders the direction, creates appropriate force to maintain neuron migration, and further participates in differentiation into apical dendrites after arrival at their final destination [29]. Normally, cortical pyramidal neurons develop one long apical dendrite and anchor the dendrite to the pial surface [30,31]. However, WDR5-deficient neurons display thin, short, and disoriented multiple apical dendrites. Moreover, they do not extend their apical dendrites to the pia. Thus, the impaired multipolar-to-bipolar transition appears to be a major factor for the polarity defect, which is the absence of the long and thick apical primary dendrite in the WDR5-deficient pyramidal neurons. WDR5-deficient neurons make dendritic branches irregularly in layer I of the cerebral cortex. Cortical layer I is a critical region to integrate neuronal circuit information from layer II/III neurons [32]. Also, layer I receives long-range inputs from multiple brain regions, including thalamic areas [33,34], as well as local inputs from GABAergic interneurons [35,36]. Abnormal dendrite architecture could contribute to neurodevelopmental and psychiatric disorders such as Down syndrome, fragile X syndrome, Angelman syndrome, Rett syndrome, autism, and schizophrenia [8,37,38]. Furthermore,

dendritic abnormalities in cortical pyramidal neurons are the most consistent pathologic correlate in intellectual disability [39]. We demonstrate that WDR5 is crucial for the polarized architecture of dendrites in upper cortical layers. Our findings provide insights into the pathogenesis underlying WDR5-associated neurodevelopmental disorders such as Kabuki syndrome and Kleefstra syndrome.

We show that WDR5 controls dendritic spine morphogenesis. WDR5-deficient neurons display a significant increase in the number of their spines. Importantly, WDR5-deficient neurons predominately form filopodia-like, immature spines. Dendritic spines are small, highly motile structures on dendritic shafts that are major sites of excitatory synapses in the brain [40]. Filopodia-like spines and thin-headed spines have been reported in some intellectual disability conditions such as human fragile-X syndrome and its mouse models [41,42]. Consistent with spine defects, WDR5-deficient neurons show abnormal excitatory synapses. Altered spine and synapse morphology connect to the changes in synaptic transmission [43,44]. Moreover, imbalance of excitatory and inhibitory synapses is correlated with disrupted neural transmission [45]. Our results indicate that WDR5 is required not only to provide a correct local environment for neural transmission via dendritic polarity but to present structural building blocks as spines for synaptogenesis. It remains to be investigated if the WDR5 effect is specific to pyramidal neurons or it broadly influences to other cell types.

Our data show that WDR5 is associated with reelin signaling in developing cortical neurons. Reelin signaling regulates neuronal migration and dendritic growth in cortical pyramidal neurons [25,46,47]. Moreover, reelin signaling induces dendrite polarity and enhancement of apical dendritic growth [48,26,49]. Our results present aberrant dendrite polarity in WDR5-deficient pyramidal neurons, which greatly resemble the dendritic morphology of multiple apical dendrites in an abnormal condition of reelin signaling [50]. Our data also show that WDR5 directly interacts with the ApoER and VldlR promoters and that WDR5-deficient neurons have reduced acetylation of Histone H3 and H4, and trimethylation of Histone H3K4 at the target gene promoters. Furthermore, lncRNA, HOTTIP modulates the interaction between WDR5 and a histone modification complex at target gene promoters. Acetylation of histone H3 is relevant to neurite outgrowth since it mediates transcriptional activation of genes associated with neurite development [51]. Methylation of H3K4 is involved in maintaining both the self-renewal and differentiation capacity of postnatal neural stem and progenitor cells [52]. lncRNAs control differentiation and self-renewal [53] and lncRNA HOTTIP recruits MLL1 through an interaction with WDR5 to distal *HOXA* genes in human fibroblasts [27]. By promoting expression of reelin signaling genes via epigenetic histone modification around those gene loci, WDR5 appears to contribute to the positioning and differentiation of pyramidal neurons. It will be interesting to elucidate whether WDR5 cooperates with BAF chromatin remodelers such as ARID1B [54] to regulate histone epigenetics and neuronal differentiation. Our data suggest a potential epigenetic mechanism responsible for cortical dendritic development.

Materials and Methods

Plasmids

shRNAs were designed by targeting a sequence (5'-GCGTGGTCATCAGATTCTAAC-3') and its complement for shWDR5 and a sequence (5'-GCACAAGCGTAGTGAAATACA-3') and its complement for shHOTTIP. These sequences were cloned into a modified pSuper-Basic vector as previously described [55,56] and pLVX-shRNA2 vector (Takara Bio). For control, non-silencing shRNAs were generated using scrambled targeting sequences (5'-GCTTACTCCCCGAGCAACATA-3' and 5'-GCCCAGACTACTCTCACAGAT-3').WDR5 coding sequence was prepared by PCR using cDNA from the mouse brain as a template. The fragment was then digested with BamHI (EcoRI) and XhoI (XbaI) (Thermo Fisher Scientific) and ligated into the overexpression vector pcDNA3.1 (Thermo Fisher Scientific). A WDR5 mutant construct that is resistant to shWDR5 was generated by site-directed mutagenesis of 12 nt at wobble positions.

Immunostaining

Immunostaining of brain sections or dissociated neural cells was performed as described previously [57,58]. The following primary antibodies were used: Mouse anti-WDR5 (Abcam, AB56919), and rabbit anti-Neu N (Abcam, AB 104225), rabbit anti-c-Myc (Abcam, AB39688), chicken anti-MAP2 (Abcam, AB5392), chicken anti-GFP (Thermo Fisher Scientific, A10262), rabbit anti-GFP (Thermo Fisher Scientific, A11122), rabbit anti-RFP (Abcam, AB62341), guinea pig anti-vGlut (EMD Millipore, AB5905), and rabbit anti-vGAT (EMD Millipore, AB5062P). Appropriate secondary antibodies conjugated with Alexa Fluor dyes (Thermo Fisher Scientific) were used to detect primary antibodies.

In utero electroporation

In utero electroporation was performed as described previously [59]. Briefly, timed pregnant female mice from E14.5 of gestation were deeply anesthetized, and the uterine horns were gently exposed by laparotomy. The lateral ventricles of an embryonic brain were injected with plasmid DNA (2 μg/μl) and 0.001% fast green (Sigma-Aldrich) using a Picospritzer II (Parker Hannifin). Electroporation was achieved by placing two sterile forceps-type electrodes on opposing sides of the uterine sac around the embryonic head and applying a series of short electrical pulses using a BTX ECM 830 electroporator (Harvard Apparatus) (five pulses with 100 ms length separated by 900 ms intervals were applied at 45 V).

Morphometry

Dendrite morphology assessment was performed as described previously [22][60]. For the quantification of lengths, numbers, or widths of GFP-positive dendrites, images of 20 different brain sections at periodic distances along the rostrocaudal axis were taken with Zeiss LSM710 confocal microscope. Ten mice were used for each experiment (control mice, $n = 5$; mutant mice, $n = 5$). Dendritic morphology in cultured neurons was also assessed with the microscope. More than 20 fields scanned horizontally and vertically were examined in each condition. Cell numbers are described in figure legends. The images were analyzed using ZEN (Zeiss), LSM image browser (Zeiss), and ImageJ. Apical dendrite lengths were

assessed from the proximal emerging point to the distal tip of an obvious apical tuft. Basal dendritic lengths were measured from the proximal branching point of a pyramidal cell base to the distal end of the basal dendrite. Apical dendrite width (thickness) was assessed at the proximal emerging point of the GFP-positive apical tuft. The calculated values were averaged, and some results were recalculated as relative changes versus control.

Primary neuron cultures

Primary neuronal culture was performed as described previously [61,62]. Briefly, cerebral cortices from E13.5–16.5 mice were isolated and dissociated with trituration after trypsin/EDTA treatment. The cells were then plated onto poly-D-lysine/ laminin-coated coverslips and cultured in a medium containing neurobasal medium, 5% serum, B27 supplements and N2 supplements.

Cell transfection

Mouse cortical neurons were transfected with various plasmids as described in previous papers [63,64]. Embryonic cortices were dissociated and suspended in 100 μl of Amaxa electroporation buffer containing 1–10 μg of plasmid DNA. Then, suspended cells were electroporated with an Amaxa Nucleofector apparatus. After electroporation, cells were plated onto coated coverslips and the medium was changed 4 hours later to remove the remnant transfection buffer. For transfecting DNA constructs into attached cells, lipofectamine (Thermo Fisher Scientific) mediated transfection was performed according to the manufacturer's protocol.

Western Blotting

Western blotting was performed as described previously [65,66]. Cellular lysates from cultured neurons were prepared using RIPA buffer. Proteins were separated on 4–12% SDS-PAGE gradient gel and transferred onto a nitrocellulose membrane. Then the membrane was incubated with rabbit anti-WDR5 (Abcam, AB56919), rabbit anti-Histone H3 (Cell signaling, #4499), rabbit anti-acetyl-Histone H3 (Abcam, AB4441), rabbit anti-acetyl-Histone H4 (Abcam, AB109463), rabbit anti-tri-methyl-Histone H3 (Lys4) (Cell signaling, #9571), rabbit anti-tri-methyl-Histone H3 (Lys4) (Cell signaling, #9754), rabbit anti-ASH2L (Protein Tech, 12331-1-AP) and rabbit anti-KANSL1 (Aviva, ARP55255_P050) antibody at 4°C overnight. Appropriate secondary antibodies conjugated to HRP were used (Cell Signaling Technology) and the ECL reagents (Thermo Fisher Scientific) were used for immunedetection. For quantification of band intensity, blots from 3 independent experiments for each molecule of interest were used. Signals were measured using Image J software and represented by relative intensity versus control. GAPDH was used as an internal control to normalize band intensity.

Reverse transcription PCR

RNA was extracted from cultured neurons using TRIZOL reagent (Thermo Fisher Scientific), and cDNA was synthesized from 1 μg of total RNA using oligo-dT and random hexamers using the Verso cDNA synthesis kit (Thermo Fisher Scientific). A measure of 1 μl of cDNA was used in reverse transcription PCR using Master Mix

(Promega Life Sciences). The sequences of the primers used were WDR5 forward 5′-CTCCTTGTGTCTGCCTCTGA-3′ and reverse 5′-GACCCTGAGACGATGAGGTT-3′, HOTTIP forward 5′- TCTGGCTCTGTTTGGTTTCTC-3′ and reverse 5′- CTAGCTGGAAAACTTCGGAGG-3′, ApoER forward 5′-CCTCATCTGGAGGAACTGGA-3′ and reverse 5′-TGCTGGTCTCCCCAAGACA-3′, VldlR forward 5′-GAAGTCAGTGTTCCCCCAAA-3′ and reverse 5′-CAGAAGCGCTGTGTCTACCA-3′, CDH2 forward 5′-GAGAGGCCTATCCATGCTGA-3′ and reverse 5′-ACCGCTACTGGAGGAGTTGA-3′, LimK forward 5′-ATGAGGTTGACGCTACTTTGTTG-3′ and reverse 5′-CTACACTCGCAACAGCACCTGAA-3′, CDK5 forward 5′-GTGACCTGGACCCTGAGATT-3′ and reverse 5′-GGGCTTCAGGTCCCTATGTA-3′, BTBD3 forward 5′-GACGGATCCAGCAATACCTT-3′ and reverse 5′-GTCACCTTGCCACACTGAAC-3′, NRG1 forward 5′-CAGCTCATCACTCCACGACT-3′ and reverse 5′-TGTGCCTGCTGTTCTCTACC-3′, NPTN forward 5′-CCAGCAACATGGAGTACAGG-3′ and reverse 5′-TCACTTCAATGGTGGCATTT-3′, AURKA forward 5′-CAGAAACTTGGAGCAGGTCA-3′ and reverse 5′-TTGTGTCTTCGGTCTTCTGC-3′, Shank3 forward 5′-ACCATCCTCAAGTCGTCCAG-3′ and reverse 5′-CACATCGAACTTGCTCCAGA-3′, GAPDH forward 5′-AAGGTCATCCCAG AGCTGAA-3′ and reverse 5′-AGGAGACAACCTGGTCCTCA-3′.

ChIP-PCR

The ChIP assay was performed using the Magna-CHIP™ A chromatin immunoprecipitation kit (EMD Millipore), followed by PCR as previously described [67]. rabbit anti-IgG (Santa Cruz Biotechnology, sc-66931), rabbit anti-WDR5 (Abcam, AB56919), or rabbit anti-acetyl-Histone H3 antibody (Abcam, AB4441) was used. The primers for amplifying the promoter regions from the precipitated fractions were 5′- AGTCAGGGGAGCAGCGGTGCG-3′ (ApoER forward), 5′-CCCCATCTCGGAGCCGCCTCT-3′ (ApoER reverse), 5′- GCACGCACGCTGCCACTTGCC-3′ (VldlR forward), 5′-GGGAACGGCGCGGGCGGCGGG-3′ (VldlR reverse), 5′-ACACCCAACCAGGTCAGAGCCG-3′ (CDK5 forward), and 5′-CCAGGAAGCATCGCGTGTCGGG-3′ (CDK5 reverse).

RNA immunoprecipitation

RNA immunoprecipitation was performed using a Magna RIP RNA-binding protein immunoprecipitation kit (EMD Millipore) according to the manufacturer's instructions. Rabbit anti-WDR5 (Abcam, AB56919), rabbit anti-ASH2L (Protein Tech, 12331-1-AP) and rabbit anti-KANSL1 (Aviva, ARP55255_P050) antibodies were used. Co-precipitated RNAs were detected by reverse transcription PCR. The primers used were HOTTIP forward 5′- TCTGGCTCTGTTTGGTTTCTC-3′ and reverse 5′-CTAGCTGGAAAACTTCGGAGG-3′.

Statistical analysis

Normal distribution was tested using Kolmogorov–Smirnov test and variance was compared. Unless otherwise stated, statistical significance was determined by two-tailed unpaired Student's t-test for two-population comparison and one/two-way analysis of variance followed by Bonferonni correction test for multiple comparisons. Data were analyzed using GraphPad Prism (GraphPad Software) and presented as mean (+/−) SEM. P values were indicated in figure legends. To determine and confirm sample sizes (N), we performed a power analysis. The values for the power (1-β) and the type I error rate (α) were 0.8 and 0.05 (or 0.01), respectively. Each experiment in this study was performed blind and randomized.

Supplementary Material

Refer to Web version on PubMed Central for supplementary material.

Funding

Research reported in this publication was supported by an award from the National Institute of Neurological Disorders and Stroke of the National Institutes of Health under award R01-NS-091220 to W.Y.K. and a grant from the National Research Foundation of Korea under grant number NRF-2019R1A2C1009006 to M.K.

Availability of data and materials

All data included in this study are available upon request by contact with the corresponding author.

References

1. Craig AM, Banker G (1994) Neuronal polarity. Annual review of neuroscience 17:267–310. doi:10.1146/annurev.ne.17.030194.001411
2. Arimura N, Kaibuchi K (2007) Neuronal polarity: from extracellular signals to intracellular mechanisms. Nature reviews Neuroscience 8 (3):194–205. doi:10.1038/nrn2056 [PubMed: 17311006]
3. Moffat JJ, Ka M, Jung EM, Kim WY (2015) Genes and brain malformations associated with abnormal neuron positioning. Molecular brain 8 (1):72. doi:10.1186/s13041-015-0164-4 [PubMed: 26541977]
4. Barnes AP, Polleux F (2009) Establishment of axon-dendrite polarity in developing neurons. Annual review of neuroscience 32:347–381. doi:10.1146/annurev.neuro.31.060407.125536
5. Jan YN, Jan LY (2010) Branching out: mechanisms of dendritic arborization. Nature reviews Neuroscience 11 (5):316–328. doi:10.1038/nrn2836 [PubMed: 20404840]
6. Bellon A (2007) New genes associated with schizophrenia in neurite formation: a review of cell culture experiments. Molecular psychiatry 12 (7):620–629. doi:10.1038/sj.mp.4001985 [PubMed: 17440437]
7. Pardo CA, Eberhart CG (2007) The neurobiology of autism. Brain pathology 17 (4):434–447. doi:10.1111/j.1750-3639.2007.00102.x [PubMed: 17919129]
8. Kaufmann WE, Moser HW (2000) Dendritic anomalies in disorders associated with mental retardation. Cerebral cortex 10 (10):981–991 [PubMed: 11007549]
9. Granato A, De Giorgio A (2014) Alterations of neocortical pyramidal neurons: turning points in the genesis of mental retardation. Frontiers in pediatrics 2:86. doi:10.3389/fped.2014.00086 [PubMed: 25157343]

10. Perissi V, Jepsen K, Glass CK, Rosenfeld MG (2010) Deconstructing repression: evolving models of co-repressor action. Nature reviews Genetics 11 (2):109–123. doi:10.1038/nrg2736
11. Kouzarides T (2007) SnapShot: Histone-modifying enzymes. Cell 131 (4):822. doi:10.1016/j.cell.2007.11.005 [PubMed: 18022374]
12. Guan JS, Haggarty SJ, Giacometti E, Dannenberg JH, Joseph N, Gao J, Nieland TJ, Zhou Y, Wang X, Mazitschek R, Bradner JE, DePinho RA, Jaenisch R, Tsai LH (2009) HDAC2 negatively regulates memory formation and synaptic plasticity. Nature 459 (7243):55–60. doi:10.1038/nature07925 [PubMed: 19424149]
13. Ang YS, Tsai SY, Lee DF, Monk J, Su J, Ratnakumar K, Ding J, Ge Y, Darr H, Chang B, Wang J, Rendl M, Bernstein E, Schaniel C, Lemischka IR (2011) Wdr5 mediates self-renewal and reprogramming via the embryonic stem cell core transcriptional network. Cell 145 (2):183–197. doi:10.1016/j.cell.2011.03.003 [PubMed: 21477851]
14. Migliori V, Mapelli M, Guccione E (2012) On WD40 proteins: propelling our knowledge of transcriptional control? Epigenetics 7 (8):815–822. doi:10.4161/epi.21140 [PubMed: 22810296]
15. Wysocka J, Swigut T, Milne TA, Dou Y, Zhang X, Burlingame AL, Roeder RG, Brivanlou AH, Allis CD (2005) WDR5 associates with histone H3 methylated at K4 and is essential for H3 K4 methylation and vertebrate development. Cell 121 (6):859–872. doi:10.1016/j.cell.2005.03.036 [PubMed: 15960974]
16. Dias J, Van Nguyen N, Georgiev P, Gaub A, Brettschneider J, Cusack S, Kadlec J, Akhtar A (2014) Structural analysis of the KANSL1/WDR5/KANSL2 complex reveals that WDR5 is required for efficient assembly and chromatin targeting of the NSL complex. Genes & development 28 (9):929–942. doi:10.1101/gad.240200.114 [PubMed: 24788516]
17. Kim JY, Yu J, Abdulkadir SA, Chakravarti D (2016) KAT8 regulates androgen signaling in prostate cancer cells. Molecular endocrinology:me20161024. doi:10.1210/me.2016-1024
18. Parisi L, Di Filippo T, Roccella M (2015) Autism spectrum disorder in Kabuki syndrome: clinical, diagnostic and rehabilitative aspects assessed through the presentation of three cases. Minerva Pediatr 67 (4):369–375 [PubMed: 26129805]
19. Eising E, Carrion-Castillo A, Vino A, Strand EA, Jakielski KJ, Scerri TS, Hildebrand MS, Webster R, Ma A, Mazoyer B, Francks C, Bahlo M, Scheffer IE, Morgan AT, Shriberg LD, Fisher SE (2019) A set of regulatory genes co-expressed in embryonic human brain is implicated in disrupted speech development. Molecular psychiatry 24 (7):1065–1078. doi:10.1038/s41380-018-0020-x [PubMed: 29463886]
20. Schulz Y, Freese L, Manz J, Zoll B, Volter C, Brockmann K, Bogershausen N, Becker J, Wollnik B, Pauli S (2014) CHARGE and Kabuki syndromes: a phenotypic and molecular link. Hum Mol Genet 23 (16):4396–4405. doi:10.1093/hmg/ddu156 [PubMed: 24705355]
21. Lee J, Zhou P (2012) Pathogenic Role of the CRL4 Ubiquitin Ligase in Human Disease. Frontiers in oncology 2:21. doi:10.3389/fonc.2012.00021 [PubMed: 22649780]
22. Ka M, Chopra DA, Dravid SM, Kim WY (2016) Essential Roles for ARID1B in Dendritic Arborization and Spine Morphology of Developing Pyramidal Neurons. The Journal of neuroscience : the official journal of the Society for Neuroscience 36 (9):2723–2742. doi:10.1523/JNEUROSCI.2321-15.2016 [PubMed: 26937011]
23. Noctor SC, Martinez-Cerdeno V, Ivic L, Kriegstein AR (2004) Cortical neurons arise in symmetric and asymmetric division zones and migrate through specific phases. Nature neuroscience 7 (2):136–144. doi:10.1038/nn1172 [PubMed: 14703572]
24. LoTurco JJ, Bai J (2006) The multipolar stage and disruptions in neuronal migration. Trends in neurosciences 29 (7):407–413. doi:10.1016/j.tins.2006.05.006 [PubMed: 16713637]
25. Niu S, Renfro A, Quattrocchi CC, Sheldon M, D'Arcangelo G (2004) Reelin promotes hippocampal dendrite development through the VLDLR/ApoER2-Dab1 pathway. Neuron 41 (1):71–84 [PubMed: 14715136]
26. Nichols AJ, Olson EC (2010) Reelin promotes neuronal orientation and dendritogenesis during preplate splitting. Cerebral cortex 20 (9):2213–2223. doi:10.1093/cercor/bhp303 [PubMed: 20064940]
27. Wang KC, Yang YW, Liu B, Sanyal A, Corces-Zimmerman R, Chen Y, Lajoie BR, Protacio A, Flynn RA, Gupta RA, Wysocka J, Lei M, Dekker J, Helms JA, Chang HY (2011) A long

noncoding RNA maintains active chromatin to coordinate homeotic gene expression. Nature 472 (7341):120–124. doi:10.1038/nature09819 [PubMed: 21423168]

28. Kriegstein AR, Noctor SC (2004) Patterns of neuronal migration in the embryonic cortex. Trends in neurosciences 27 (7):392–399. doi:10.1016/j.tins.2004.05.001 [PubMed: 15219738]
29. Marin O, Valiente M, Ge X, Tsai LH (2010) Guiding neuronal cell migrations. Cold Spring Harbor perspectives in biology 2 (2):a001834. doi:10.1101/cshperspect.a001834 [PubMed: 20182622]
30. Ito M, Kato M, Kawabata M (1998) Premature bifurcation of the apical dendritic trunk of vibrissa-responding pyramidal neurones of X-irradiated rat neocortex. The Journal of physiology 512 (Pt 2):543–553 [PubMed: 9763642]
31. Spruston N (2008) Pyramidal neurons: dendritic structure and synaptic integration. Nature reviews Neuroscience 9 (3):206–221. doi:10.1038/nrn2286 [PubMed: 18270515]
32. Lee SH, Kwan AC, Dan Y (2014) Interneuron subtypes and orientation tuning. Nature 508 (7494):E1–2. doi:10.1038/nature13128 [PubMed: 24695313]
33. Cauller L (1995) Layer I of primary sensory neocortex: where top-down converges upon bottom-up. Behavioural brain research 71 (1–2):163–170 [PubMed: 8747184]
34. Rubio-Garrido P, Perez-de-Manzo F, Porrero C, Galazo MJ, Clasca F (2009) Thalamic input to distal apical dendrites in neocortical layer 1 is massive and highly convergent. Cerebral cortex 19 (10):2380–2395. doi:10.1093/cercor/bhn259 [PubMed: 19188274]
35. Schwartzkroin PA (1998) GABA synapses enter the molecular big time. Nature medicine 4 (10):1115–1116. doi:10.1038/2608
36. Soda T, Nakashima R, Watanabe D, Nakajima K, Pastan I, Nakanishi S (2003) Segregation and coactivation of developing neocortical layer 1 neurons. The Journal of neuroscience : the official journal of the Society for Neuroscience 23 (15):6272–6279 [PubMed: 12867512]
37. Zoghbi HY (2003) Postnatal neurodevelopmental disorders: meeting at the synapse? Science 302 (5646):826–830. doi:10.1126/science.1089071 [PubMed: 14593168]
38. Walsh CA, Morrow EM, Rubenstein JL (2008) Autism and brain development. Cell 135 (3):396–400. doi:10.1016/j.cell.2008.10.015 [PubMed: 18984148]
39. Belichenko PV, Wright EE, Belichenko NP, Masliah E, Li HH, Mobley WC, Francke U (2009) Widespread changes in dendritic and axonal morphology in Mecp2-mutant mouse models of Rett syndrome: evidence for disruption of neuronal networks. The Journal of comparative neurology 514 (3):240–258. doi:10.1002/cne.22009 [PubMed: 19296534]
40. Harris KM, Kater SB (1994) Dendritic spines: cellular specializations imparting both stability and flexibility to synaptic function. Annual review of neuroscience 17:341–371. doi:10.1146/annurev.ne.17.030194.002013
41. Irwin SA, Idupulapati M, Gilbert ME, Harris JB, Chakravarti AB, Rogers EJ, Crisostomo RA, Larsen BP, Mehta A, Alcantara CJ, Patel B, Swain RA, Weiler IJ, Oostra BA, Greenough WT (2002) Dendritic spine and dendritic field characteristics of layer V pyramidal neurons in the visual cortex of fragile-X knockout mice. American journal of medical genetics 111 (2):140–146. doi:10.1002/ajmg.10500 [PubMed: 12210340]
42. McKinney BC, Grossman AW, Elisseou NM, Greenough WT (2005) Dendritic spine abnormalities in the occipital cortex of C57BL/6 Fmr1 knockout mice. American journal of medical genetics Part B, Neuropsychiatric genetics : the official publication of the International Society of Psychiatric Genetics 136B (1):98–102. doi:10.1002/ajmg.b.30183
43. Matsuzaki M, Honkura N, Ellis-Davies GC, Kasai H (2004) Structural basis of long-term potentiation in single dendritic spines. Nature 429 (6993):761–766. doi:10.1038/nature02617 [PubMed: 15190253]
44. Tropea D, Majewska AK, Garcia R, Sur M (2010) Structural dynamics of synapses in vivo correlate with functional changes during experience-dependent plasticity in visual cortex. The Journal of neuroscience : the official journal of the Society for Neuroscience 30 (33):11086–11095. doi:10.1523/JNEUROSCI.1661-10.2010 [PubMed: 20720116]
45. Gatto CL, Broadie K (2010) Genetic controls balancing excitatory and inhibitory synaptogenesis in neurodevelopmental disorder models. Frontiers in synaptic neuroscience 2:4. doi:10.3389/fnsyn.2010.00004 [PubMed: 21423490]

46. Franco SJ, Martinez-Garay I, Gil-Sanz C, Harkins-Perry SR, Muller U (2011) Reelin regulates cadherin function via Dab1/Rap1 to control neuronal migration and lamination in the neocortex. Neuron 69 (3):482–497. doi:10.1016/j.neuron.2011.01.003 [PubMed: 21315259]
47. Sekine K, Kawauchi T, Kubo K, Honda T, Herz J, Hattori M, Kinashi T, Nakajima K (2012) Reelin controls neuronal positioning by promoting cell-matrix adhesion via inside-out activation of integrin alpha5beta1. Neuron 76 (2):353–369. doi:10.1016/j.neuron.2012.07.020 [PubMed: 23083738]
48. Matsuki T, Matthews RT, Cooper JA, van der Brug MP, Cookson MR, Hardy JA, Olson EC, Howell BW (2010) Reelin and stk25 have opposing roles in neuronal polarization and dendritic Golgi deployment. Cell 143 (5):826–836. doi:10.1016/j.cell.2010.10.029 [PubMed: 21111240]
49. O'Dell RS, Ustine CJ, Cameron DA, Lawless SM, Williams RM, Zipfel WR, Olson EC (2012) Layer 6 cortical neurons require Reelin-Dab1 signaling for cellular orientation, Golgi deployment, and directed neurite growth into the marginal zone. Neural development 7:25. doi:10.1186/1749-8104-7-25 [PubMed: 22770513]
50. Ohshima T, Hirasawa M, Tabata H, Mutoh T, Adachi T, Suzuki H, Saruta K, Iwasato T, Itohara S, Hashimoto M, Nakajima K, Ogawa M, Kulkarni AB, Mikoshiba K (2007) Cdk5 is required for multipolar-to-bipolar transition during radial neuronal migration and proper dendrite development of pyramidal neurons in the cerebral cortex. Development 134 (12):2273–2282. doi:10.1242/dev.02854 [PubMed: 17507397]
51. Tomioka T, Maruoka H, Kawa H, Yamazoe R, Fujiki D, Shimoke K, Ikeuchi T (2014) The histone deacetylase inhibitor trichostatin A induces neurite outgrowth in PC12 cells via the epigenetically regulated expression of the nur77 gene. Neuroscience research 88:39–48. doi:10.1016/j.neures.2014.07.009 [PubMed: 25128386]
52. Shah K, King GD, Jiang H (2020) A chromatin modulator sustains self-renewal and enables differentiation of postnatal neural stem and progenitor cells. J Mol Cell Biol 12 (1):4–16. doi:10.1093/jmcb/mjz036 [PubMed: 31065682]
53. Flynn RA, Chang HY (2014) Long noncoding RNAs in cell-fate programming and reprogramming. Cell Stem Cell 14 (6):752–761. doi:10.1016/j.stem.2014.05.014 [PubMed: 24905165]
54. Moffat JJ, Jung EM, Ka M, Smith AL, Jeon BT, Santen GWE, Kim WY (2019) The role of ARID1B, a BAF chromatin remodeling complex subunit, in neural development and behavior. Progress in neuro-psychopharmacology & biological psychiatry 89:30–38. doi:10.1016/j.pnpbp.2018.08.021 [PubMed: 30149092]
55. Kim WY, Zhou FQ, Zhou J, Yokota Y, Wang YM, Yoshimura T, Kaibuchi K, Woodgett JR, Anton ES, Snider WD (2006) Essential roles for GSK-3s and GSK-3-primed substrates in neurotrophin-induced and hippocampal axon growth. Neuron 52 (6):981–996. doi:10.1016/j.neuron.2006.10.031 [PubMed: 17178402]
56. Ka M, Jung EM, Mueller U, Kim WY (2014) MACF1 regulates the migration of pyramidal neurons via microtubule dynamics and GSK-3 signaling. Developmental biology 395 (1):4–18. doi:10.1016/j.ydbio.2014.09.009 [PubMed: 25224226]
57. Kim WY, Wang X, Wu Y, Doble BW, Patel S, Woodgett JR, Snider WD (2009) GSK-3 is a master regulator of neural progenitor homeostasis. Nature neuroscience 12 (11):1390–1397. doi:10.1038/nn.2408 [PubMed: 19801986]
58. Ka M, Smith AL, Kim WY (2017) MTOR controls genesis and autophagy of GABAergic interneurons during brain development. Autophagy:1–16. doi:10.1080/15548627.2017.1327927
59. Ka M, Kim WY (2018) ANKRD11 associated with intellectual disability and autism regulates dendrite differentiation via the BDNF/TrkB signaling pathway. Neurobiology of disease 111:138–152. doi:10.1016/j.nbd.2017.12.008 [PubMed: 29274743]
60. Ledergerber D, Larkum ME (2010) Properties of layer 6 pyramidal neuron apical dendrites. The Journal of neuroscience : the official journal of the Society for Neuroscience 30 (39):13031–13044. doi:10.1523/JNEUROSCI.2254-10.2010 [PubMed: 20881121]
61. Kim WY, Horbinski C, Sigurdson W, Higgins D (2004) Proteasome inhibitors suppress formation of polyglutamine-induced nuclear inclusions in cultured postmitotic neurons. Journal of neurochemistry 91 (5):1044–1056. doi:10.1111/j.1471-4159.2004.02788.x [PubMed: 15569248]

62. Ka M, Kook YH, Liao K, Buch S, Kim WY (2016) Transactivation of TrkB by Sigma-1 receptor mediates cocaine-induced changes in dendritic spine density and morphology in hippocampal and cortical neurons. Cell death & disease 7 (10):e2414. doi:10.1038/cddis.2016.319 [PubMed: 27735948]

63. Ka M, Condorelli G, Woodgett JR, Kim WY (2014) mTOR regulates brain morphogenesis by mediating GSK3 signaling. Development 141 (21):4076–4086. doi:10.1242/dev.108282 [PubMed: 25273085]

64. Ka M, Moffat JJ, Kim WY (2017) MACF1 Controls Migration and Positioning of Cortical GABAergic Interneurons in Mice. Cerebral cortex 27 (12):5525–5538. doi:10.1093/cercor/bhw319 [PubMed: 27756764]

65. Ka M, Kim WY (2016) Microtubule-Actin Crosslinking Factor 1 Is Required for Dendritic Arborization and Axon Outgrowth in the Developing Brain. Molecular neurobiology 53 (9):6018–6032. doi:10.1007/s12035-015-9508-4 [PubMed: 26526844]

66. Jung EM, Ka M, Kim WY (2016) Loss of GSK-3 Causes Abnormal Astrogenesis and Behavior in Mice. Molecular neurobiology 53 (6):3954–3966. doi:10.1007/s12035-015-9326-8 [PubMed: 26179612]

67. Jung EM, Moffat JJ, Liu J, Dravid SM, Gurumurthy CB, Kim WY (2017) Arid1b haploinsufficiency disrupts cortical interneuron development and mouse behavior. Nature neuroscience 20 (12):1694–1707. doi:10.1038/s41593-017-0013-0 [PubMed: 29184203]

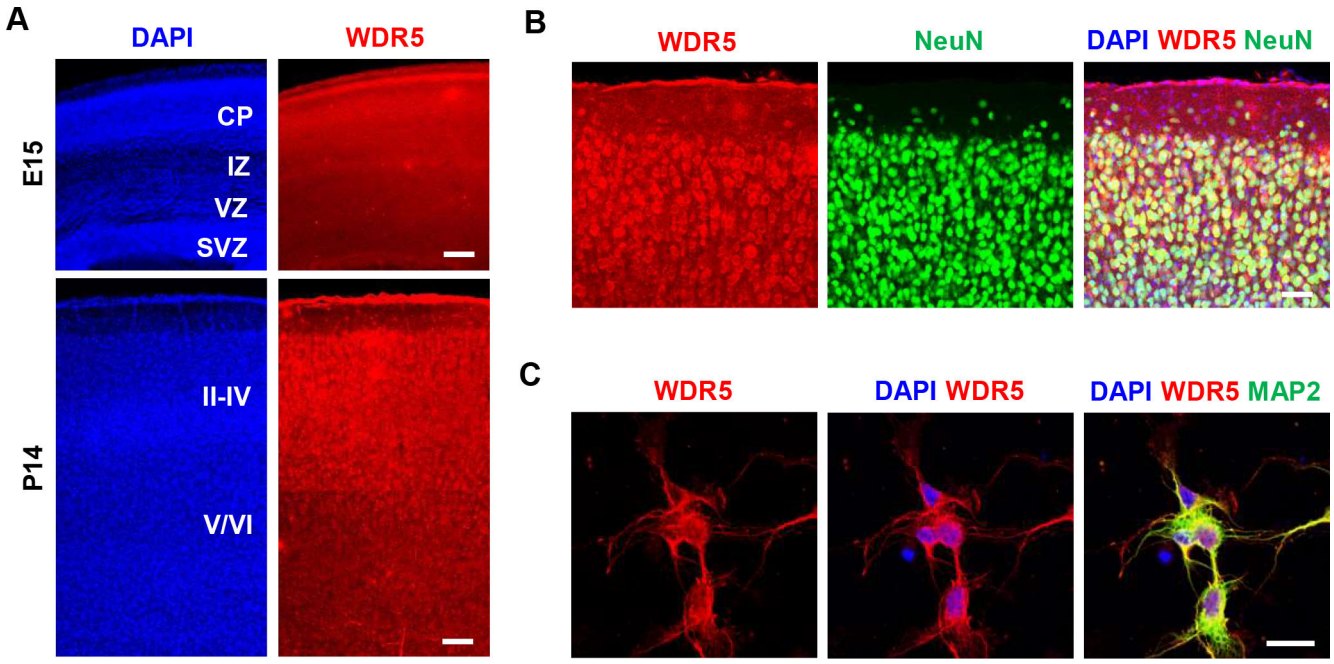

Figure 1. Expression patterns of WDR5 in the developing cortex

(A) Expression of WDR5 in embryonic and postnatal mouse brains. Immunostaining for WDR5 showed that the protein was broadly expressed in the embryonic mouse brains. In postnatal mouse brains, WDR5 was highly expressed in the upper-layer cortical plate. Scale bar, 50μm, 150μm. CP, Cortical plate; IZ, intermediate zone, VZ, ventricular zone, SVZ, subventricular zone; II-VI, cortical layers II-VI. (B) WDR5 immunostaining in NeuN-positive cells in postnatal mouse brains. WDR5 was highly expressed in upper-layer cortical neurons at P14, suggesting roles for WDR5 in neuron differentiation. Scale bar, 25μm. (C) WDR5 immunostaining in MAP2-positive neurons in culture. Scale bar, 10μm.

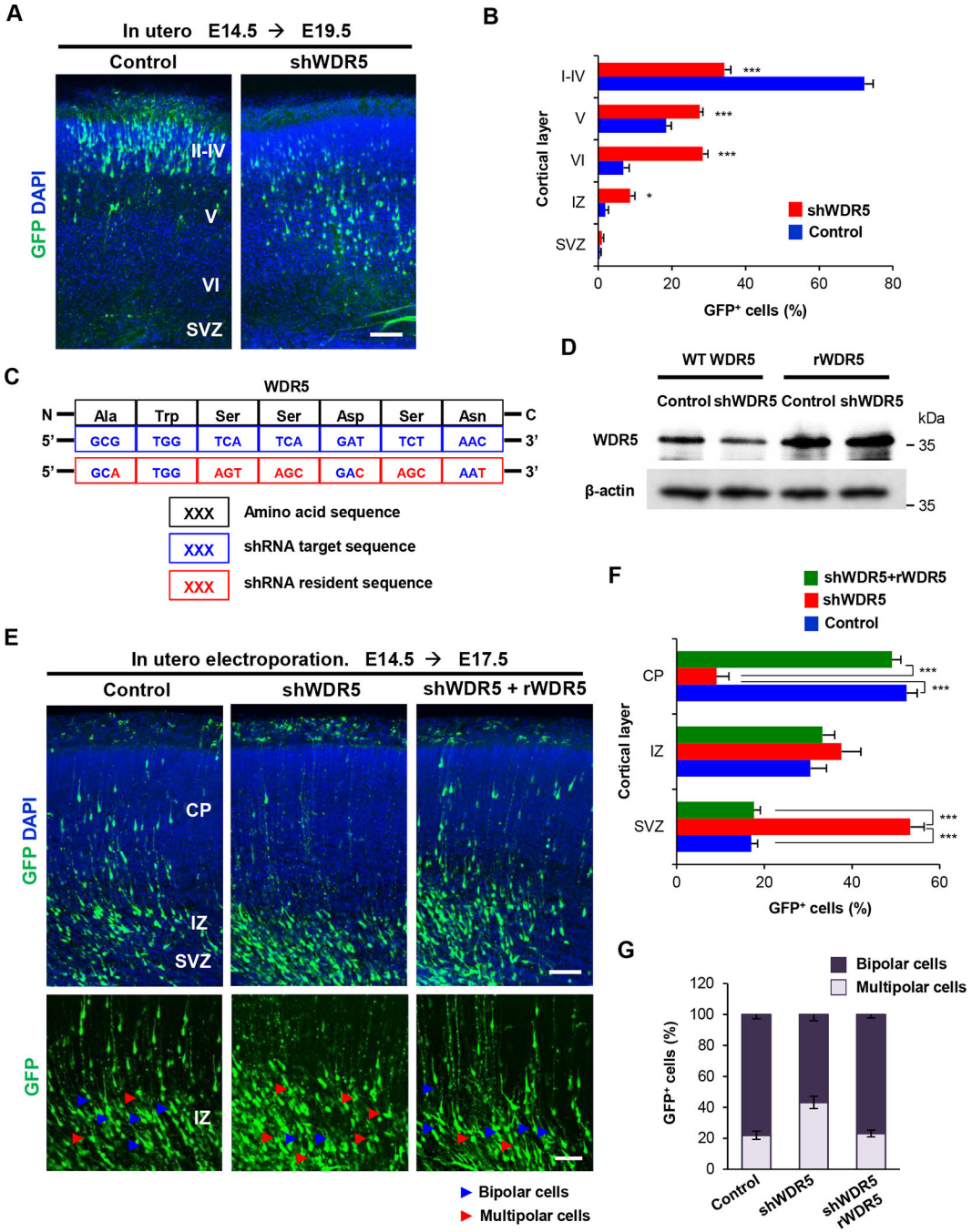

Figure 2. WDR5-suppressed neurons exhibit a defect in neuronal migration to the cortical Plate

(A) shRNA-mediated WDR5-supression induced abnormal localization of electroporated cells in the brain. E14.5 mouse brains were electroporated *in utero* with nonsilencing shRNA (control) or shWDR5 construct. shRNAs encoded GFP in a separate reading frame for a labeling purpose. The brain samples were collected at E19.5 stages. GFP-positive or RFP-positive cells were visualized in the lateral cerebral cortex. Scale bar, 50μm. (B) Quantification of neuron positions throughout the cerebral cortex. n=5 mice for each condition. Statistical significance was determined by two-way ANOVA with Bonferonni

correction test. Data shown are mean (+/−) SEM. Stars indicate significant difference when compared with controls. *$p < 0.05$, ***$p < 0.001$. (C) Illustration showing the silent mutations in the shWDR5-resistant construct of WDR5. The twelve silent mutations (red) in the shWDR5-target sequence (blue) of the WT WDR5 amino acids (black), which confer resistance to the shWDR5 and no change in the amino acid sequence compared with the WT WDR5. (D) Western blot showing insensitivity of rWDR5 versus sensitivity of WT WDR5 to shWDR5. The proteins were exogenously expressed in HEK 293T cells. n=3 independent experiments for WDR5 expression in HEK 293T cells. (E) Co-expression of rWDR5 construct restored the inhibitory effect of shWDR5 in pyramidal neural migration. Control shRNA or shWDR5 or shWDR5 with rWDR5 plasmid were electroporated *in utero* into E14.5 mouse embryos and observed neural migration and multipolar to bipolar transition of pyramidal neurons at E17.5. Scale bar, 50μm, 25μm. (F) Quantification of neuron positions throughout the cerebral cortex. n=5 mice for each condition. Statistical significance was determined by two-way ANOVA with Bonferonni correction test. Data shown are mean (+/−) SEM. Stars indicate significant difference when compared with controls. ***$p < 0.001$. (G) Co-expression of rWDR5 construct rescued the inhibitory effect of shWDR5 in multipolar to bipolar transition. Quantification of numbers either multipolar or bipolar neurons in IZ. n=5 mice for each condition. Statistical significance was determined by two-way ANOVA with Bonferonni correction test.

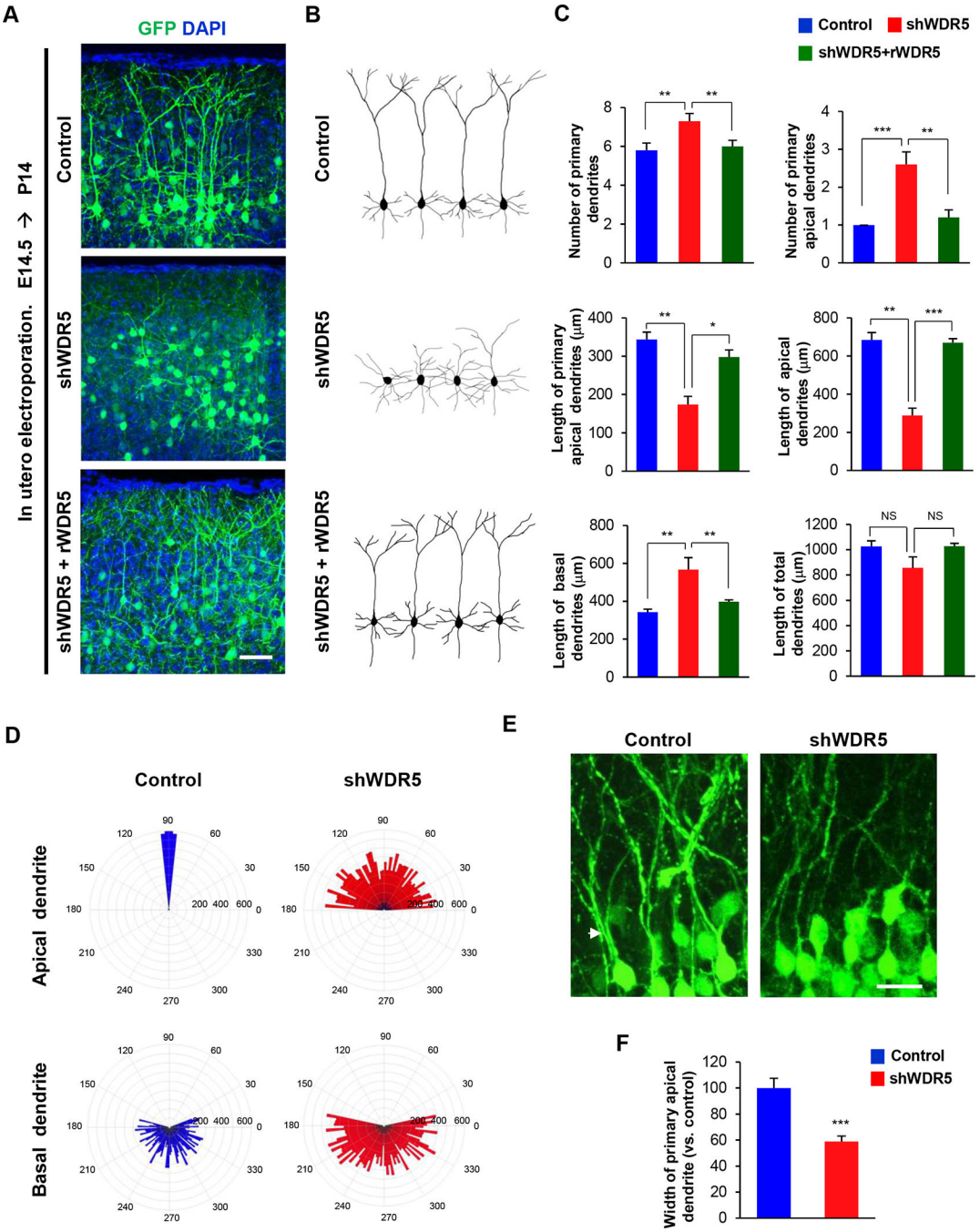

Figure 3. WDR5 regulates dendritic polarity of cortical pyramidal neurons.

(A) Knockdown of WDR5 inhibits primary apical dendrite development in pyramidal neurons, and co-expression of rWDR5 construct restored the inhibitory effect of shWDR5. E14.5 embryos were electroporated *in utero* with a control or shWDR5 or shWDR5 and rWDR5 construct to target cortical pyramidal neurons. The electroporated brains were collected at age P14 and dendrite morphologies in pyramidal neurons expressing GFP were visualized. Scale bar, 25μm. (B) Representative morphologies of control, shWDR5 or shWDR5 + rWDR5-expressing pyramidal neurons with their dendrite formation. (C) The

numbers and lengths of dendrites were quantified. n=5 mice for each condition. Statistical significance was determined by one-way ANOVA with Bonferonni correction test. *$p <$ 0.05, **$p < 0.01$, ***$p < 0.001$. (D) Knockdown of WDR5 shows abnormal orientation of apical dendrites in pyramidal neurons. The numbers on the outer circle indicate the degrees of angles from the right horizontal line. The numbers inside of the outer circle show the lengths of dendrites. n=50 cells from 5 mice for each condition. (E) Knockdown of WDR5 shows thin primary apical dendrite in pyramidal neurons. Arrowheads show the primary apical dendrite of pyramidal neurons. Scale bar, 10μm. (F) The width of main apical dendrites was quantified. n=5 mice for each condition. Statistical significance was determined by two-tailed Student's t-test. ***$p < 0.001$.

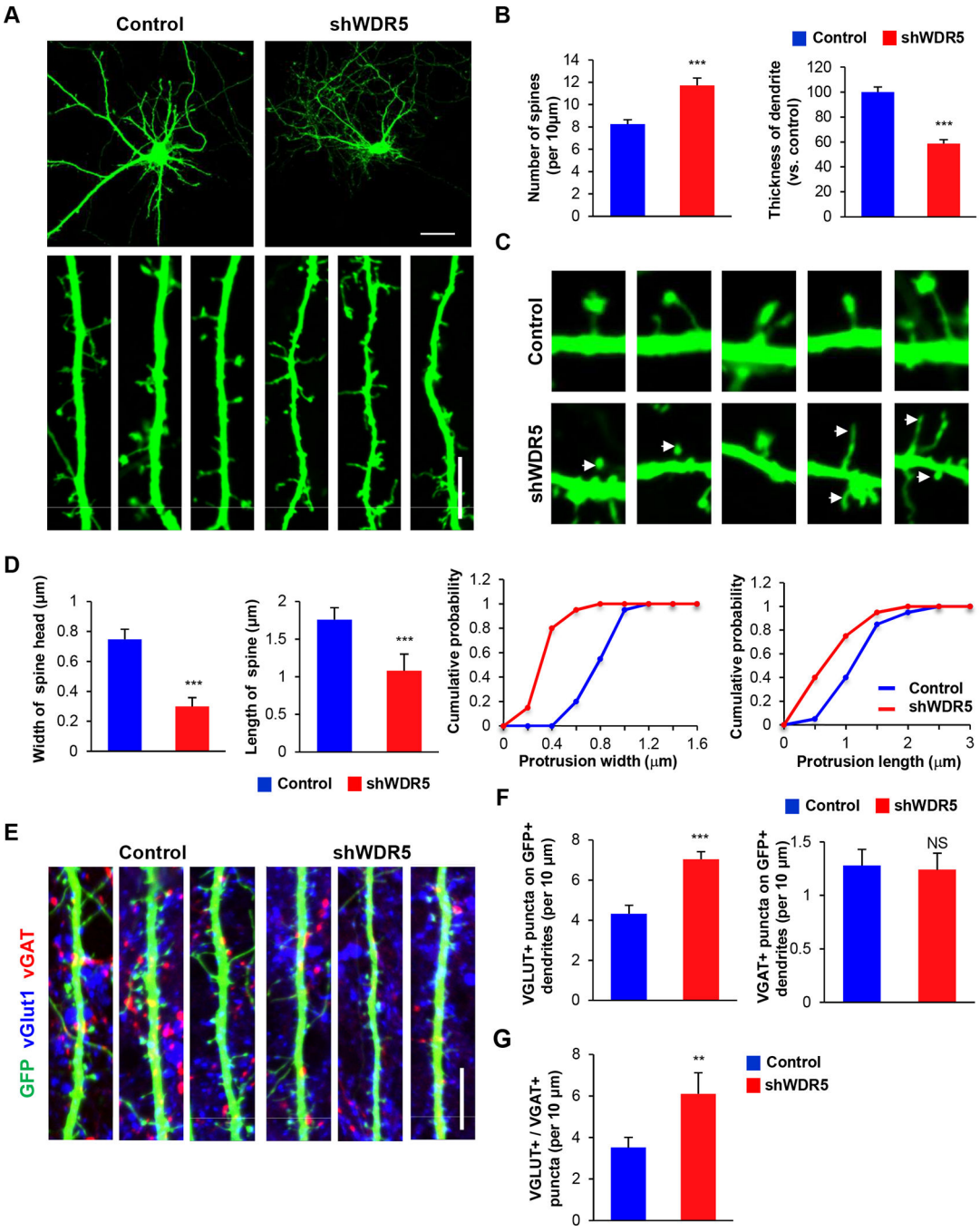

Figure 4. Knockdown of WDR5 leads to abnormal formation of dendrite and dendritic spines.

(A) WDR5-suppressed neurons exhibited decreased width of secondary dendrites, however, the number of dendritic spines did not appear to be different between control and WDR5-suppressed neurons. Cortical neurons from E15.5 mice were cultured for 14 d after transfecting them with control shRNA or shWDR5. Scale bar, 25μm, 5μm. (B) The width of secondary dendrites and the number of dendritic spines was quantified. n=100 dendrites from 30 primary cultured cortical neurons for either control and WDR5-suppressed neurons. Statistical significance was determined by two-tailed Student's t-test. ***$p < 0.001$. (C)

Higher magnification images of dendritic spines. WDR5-supressed neurons show aberrant dendritic spines. Arrowheads show the dendritic spines in secondary dendrites of cultured cortical neurons. (D) The lengths, and sizes of spines were quantified. n=45 cells from 3 independent cultures using 3 mice. Statistical significance was determined by two-tailed Student's t-test. ***$p < 0.001$. (E) Knockdown of WDR5 reduces the number of excitatory and inhibitory synapses. Excitatory and inhibitory synapses were assessed by immunostaining with vGlut1 and vGAT antibodies. Scale bar, 5μm. (F) The numbers of synapses were quantified. n=45 cells from three independent cultures using three mice. Statistical significance was determined by two-tailed Student's t-test. ***$p < 0.001$. (G) Knockdown of WDR5 changes the balance of excitatory and inhibitory synaptic puncta. n=45 cells from 3 independent cultures using 3 mice. Statistical significance was determined by two-tailed Student's t-test. ** P<0.01.

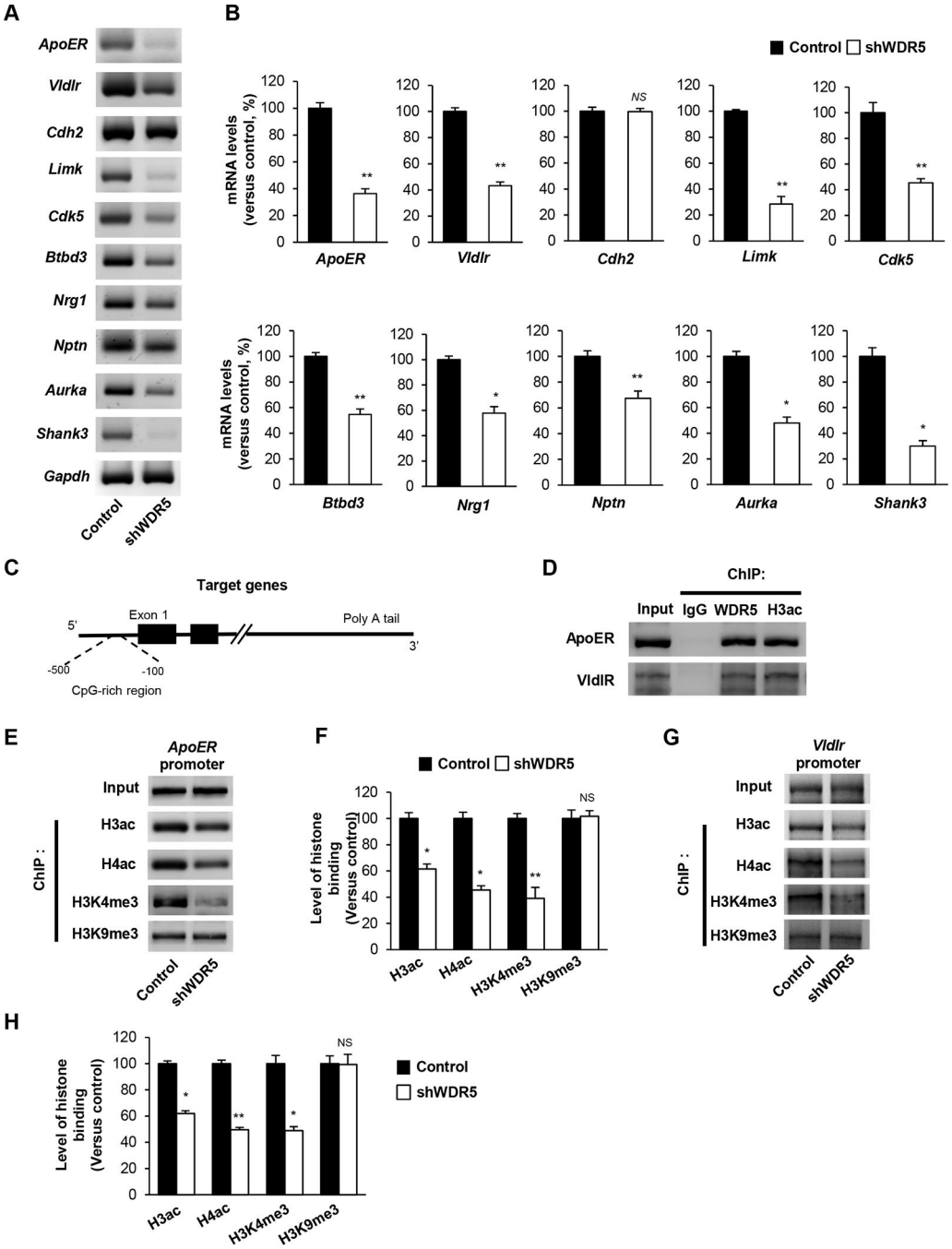

Figure 5. WDR5 regulates reelin signaling via regulating reelin signaling components expression

(A) Knockdown of WDR5 decreases the transcript levels of Reelin signaling components and neurite development related genes. Cortical neurons from E15.5 mice were cultured and infected with a lentivirus encording control or shWDR5 at 5 DIV. Cellular lysates from the cultures at 14 DIV were subjected to RNA isolation and RT-PCR. (B) Quantification of transcript levels of (A). The relative levels of the genes were normalized to GAPDH expression. The band intensities were measured using Image J software. n=3 independent primary cultured cortical neurons using 3 mice. Statistical significance was determined

by two-tailed Student's t-test. *$p < 0.05$, **$p < 0.01$. (C) Illustration showing the CHIP assay of target gene promoter region. (D) WDR5 directly interacts with ApoER, VldlR and CDK5 gene promoter. ChIP assays were performed using primary cultured neurons. (E), (G) WDR5 suppression significantly decrease the level of acetylated Histone H3 at the target genes promoter. (F), (H) Quantification of (E), (G). The relative levels of the fold change were normalized to input fraction of Acetyl-histone H3 levels at the target genes promoter. n=3 independent primary cultured cortical neurons using 3 mice. Statistical significance was determined by two-tailed Student's t-test. *$p < 0.05$, **$p < 0.01$.

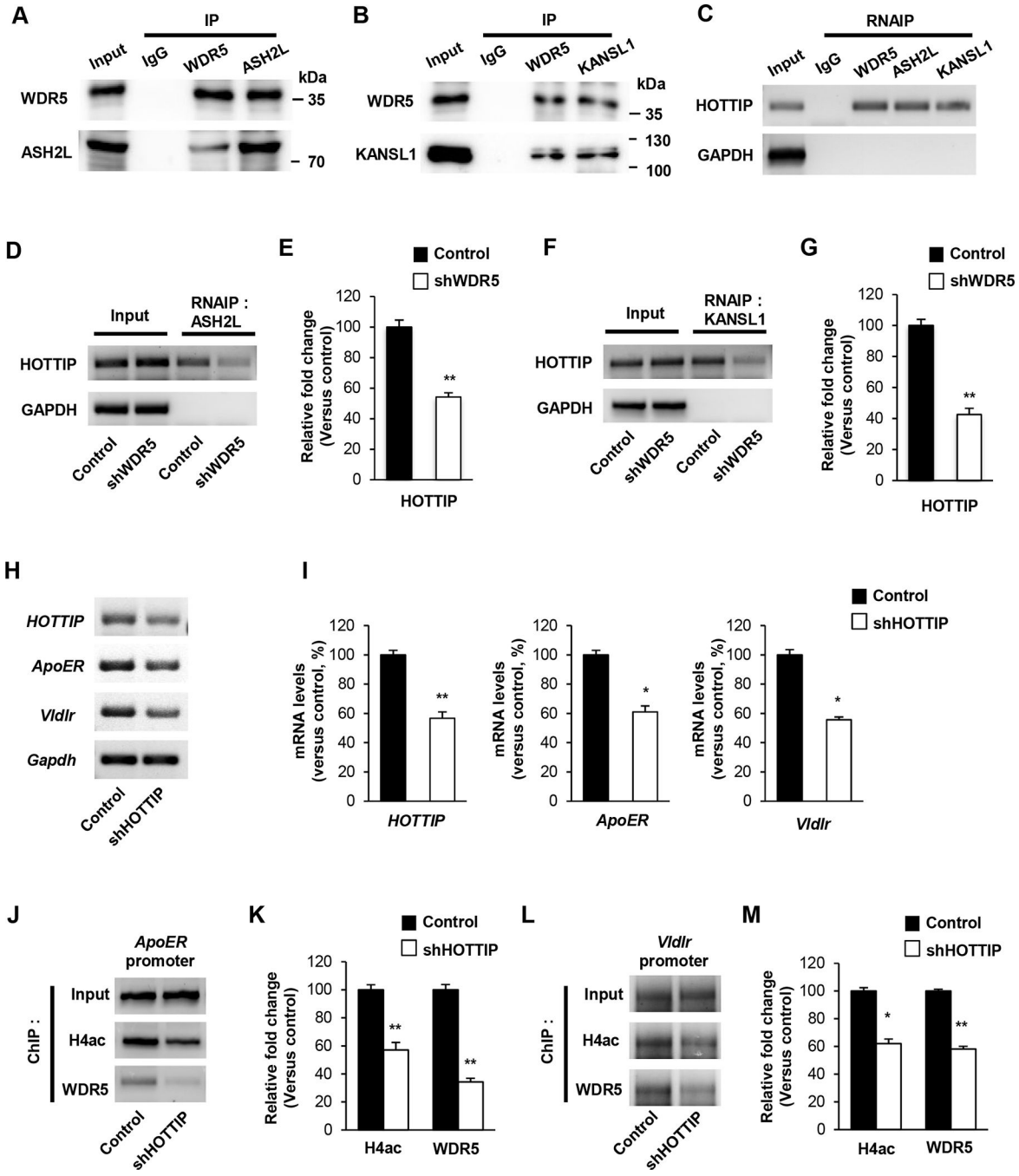

Figure 6. WDR5 regulates histone modification via interact with histone modification complex and lnc RNA, HOTTIP

(A) WDR5 and histone modification complexes interact with lnc RNA, HOTTIP. RNAIP assays were performed using P14 brain lysates. (B) WDR5 interacts with H3K4 methyltransferase component, ASL2L. IP assays were performed using P14 brain lysates. (C) WDR5 binds with Histone H4 acetyltransferase component, KANSL1. IP assays were performed using P14 brain lysates. (D), (F) Knockdown of WDR5 reduces interaction of lnc RNA, HOTTIP and ASH2L or KANSL1. Cortical neurons from E15.5 mice were cultured and infected with a lentivirus encoding control or shWDR5 at 5 DIV. Cellular

lysates from the cultures at 7 DIV were subjected to RNAIP assays. (E), (G) Quantification of transcript levels of (D), (F). The relative levels of the fold change were normalized to input fraction of HOTTIP and GAPDH. n=3 independent primary cultured cortical neurons using 3 mice. Statistical significance was determined by two-tailed Student's t-test. *$p <$ 0.05, **$p < 0.01$. (H) Knockdown of HOTTIP decreases the transcript levels of ApoER, VldlR and CDK5 genes. Cortical neurons from E15.5 mice were cultured and infected with a lentivirus encording control or shHOTTIP at 5 DIV. Cellular lysates from the cultures at 14 DIV were subjected to RNA isolation and RT-PCR. (I) Quantification of transcript levels of (H). The relative levels of the transcripts were normalized to GAPDH expression. The band intensities were measured using Image J software. n=3 independent primary cultured cortical neurons using 3 mice. Statistical significance was determined by two-tailed Student's t-test. *$p < 0.05$,**$p < 0.01$. (J), (L) HOTTIP suppression significantly decreases the level of WDR5 and acetylated Histone H4 at the target genes promoter. (K), (M) Quantification of (J), (L). The relative levels of the fold change were normalized to input fraction of Acetyl-histone H3 levels at the target genes promoter. n=3 independent primary cultured cortical neurons using 3 mice. Statistical significance was determined by two-tailed Student's t-test. *$p < 0.05$, **$p < 0.01$.

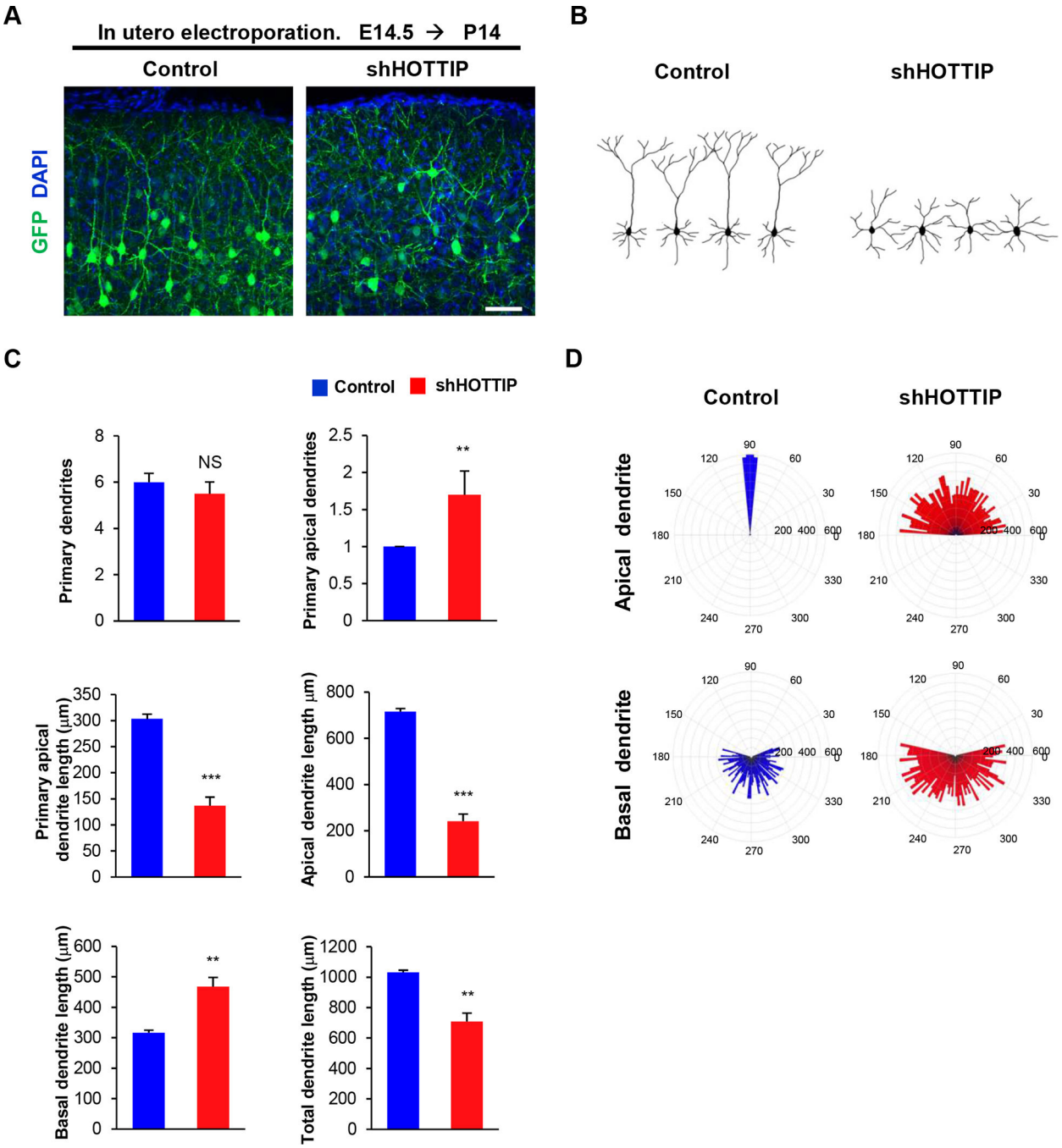

Figure 7. lnc RNA, HOTTIP regulates dendritic polarity of cortical pyramidal neurons.

(A) Knockdown of HOTTIP inhibits primary apical dendrite development in pyramidal neurons. E14.5 embryos were electroporated *in utero* with a control or shHOTTIP construct to target cortical pyramidal neurons. The electroporated brains were collected at age P14 and dendrite morphologies in pyramidal neurons expressing GFP were visualized. Scale bar, 25μm. (B) Representative morphologies of control or shHOTTIP-expressing pyramidal neurons with their dendrite formation. (C) The numbers and lengths of dendrites were quantified. n=5 mice for each condition. Statistical significance was determined by two-

tailed Student's t-test. $^{**}p < 0.01$, $^{***}p < 0.001$. (D) Knockdown of HOTTIP shows abnormal orientation of apical dendrites in pyramidal neurons. The numbers on the outer circle indicate the degrees of angles from the right horizontal line. The numbers inside of the outer circle show the lengths of dendrites. n=50 cells from 5 mice for each condition. Statistical significance was determined by two-tailed Student's t-test. $^{***}p < 0.001$.

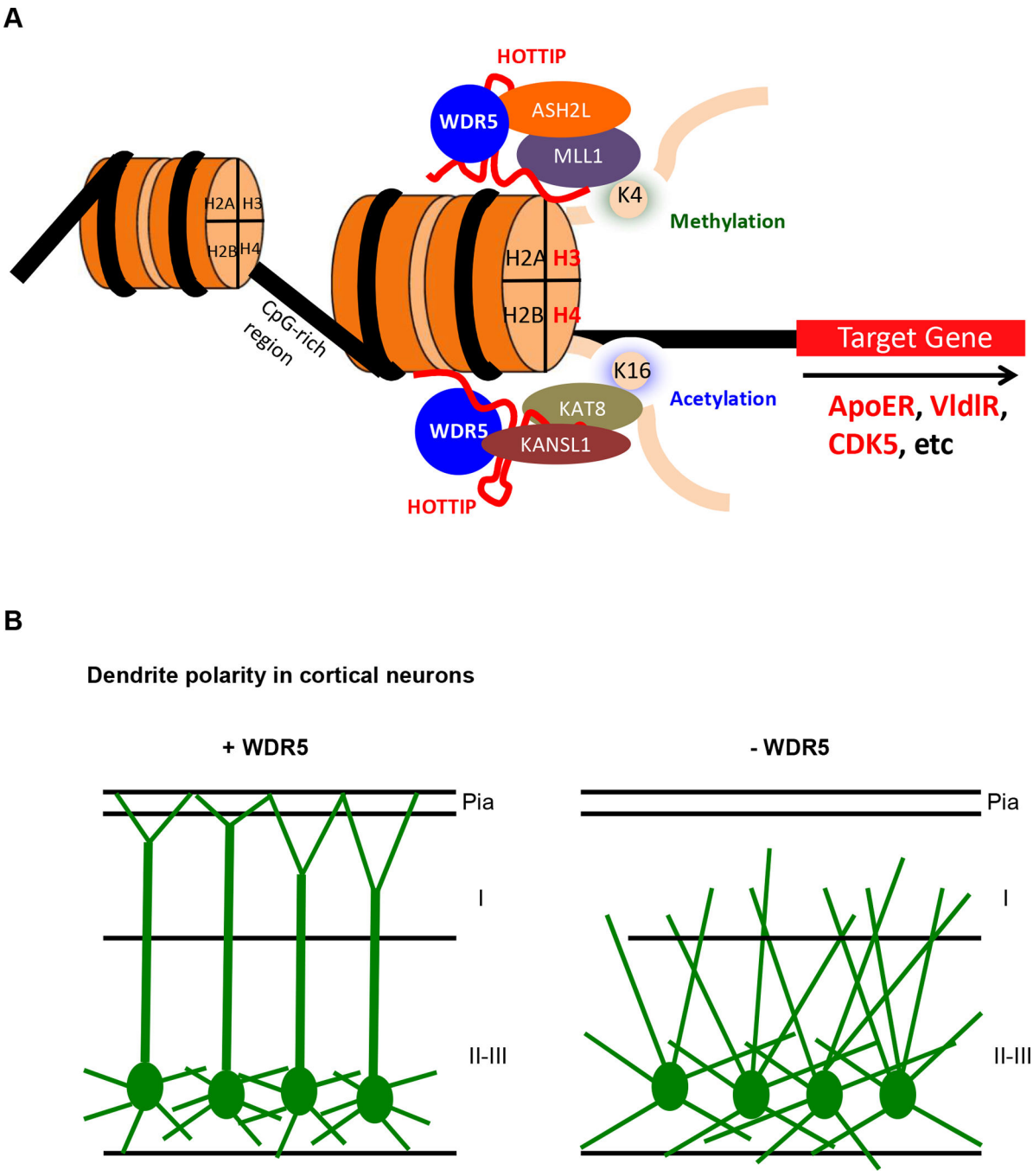

Figure 8. A schematic model illustrating a role of WDR5 in dendrite polarity

(A) A schematic model of target gene regulation of WDR5. WDR5 interact with lnc RNA, HOTTIP and histone modification complexes and regulation of target gene transcription. (B) WDR5 regulates apical dendrite polarity and extension. Control neurons elongate single long apical dendrite toward the pial surface and branching their dendrites nearby pial surface. In contrast, WDR5-suppressed neurons develop multiple apical dendrites and branched irregularly their dendrite in cortical layer I